

## Supporting Information

# Visible Light Photoactivity from Bonding Assembly of Titanium Oxide Nanocrystals

Hua Tong, Naoto Umezawa and Jinhua Ye\*

*International Center for Materials Nanoarchitectonics (MANA), and Photocatalytic  
Materials Center, National Institute for Materials Science (NIMS), 1-2-1 Sengen,  
Tsukuba, Ibaraki 305-0047, Japan. \*E-mail: Jinhua.YE@nims.go.jp*

### 1. Synthetic procedure

The TiO<sub>2</sub> NCs were synthesized by a microwave assisted solvothermal method. In a typical synthesis, TiCl<sub>4</sub> (1 mL) was dropped into absolute ethanol (2.5 mL) in a beaker with magnetic stirring (note: for safety this operation must be done under ventilation condition), then addition of benzyl alcohol (47.5 mL) was followed to form a clear precursor solution with slight green-yellow color. The precursor solution was transferred into an autoclave and treated in a microwave reactor (Microwave Laboratory System, Milestone General, Japan) following a program of heating to 160 °C in 5 minutes and keeping temperature at 160 °C for 10 minutes. After the solution cooling down, the solid product (TiO<sub>2</sub> NCs) was separated out by centrifugation. In order to remove the benzyl alcohol, the TiO<sub>2</sub> NCs were washed with absolute ethanol in a supersonic bath and purified by centrifugation for at least three cycles. Then the TiO<sub>2</sub> NCs were redispersed into 50 mL absolute ethanol and laid with heating at ~60 °C and magnetic stirring for 24 h. After that, washing with absolute ethanol in an ultrasonic bath and purifying by centrifugation for TiO<sub>2</sub> nanocrystals were repeated for at least three times. For assembly of TiO<sub>2</sub> NCs, one piece of above prepared TiO<sub>2</sub>NCs was well ultrasonically dispersed in 20 mL absolute ethanol, and then was placed in a drying box at 70 °C for 72 h and at 100 °C for 2h.

### 2. Facilities information

The prepared samples were characterized by X-ray diffraction (Cu K $\alpha$  radiation, JEOL JDX-3500, Japan), UV-visible diffuse reflectance spectra (UV-2500PC, Shimadzu, Japan), SEM (JSM-6701F, JEOL, Japan), EDS (JED-2300 Energy Dispersive X-ray Analyzer, JEOL, Japan), TEM (JEM-2100, JEOL, Japan). XPS (X-ray: Mono Al 10mA $\times$ 15KV, PE: 40 eV, Kratos Axis Ultra DLD, Shimadzu), Raman spectra (NRS-1000 Laser Raman Spectrophotometer; Jasco Inc., Japan), IR (IR Prestige-21 Fourier Transform Infrared Spectrophotometer; Shimadzu Corp., Japan).

### 3. Photocatalytic evaluation of materials

The test of photocatalytic decomposition of 2-propanol into CO<sub>2</sub> over the assembled TiO<sub>2</sub> nanocrystals, crushed powder and commercial TiO<sub>2</sub> materials, including anatase (Wako), N-doped anatase (TPS-201) and P25 (Degussa) was done in a cylindrical air-filled static Pyrex glass vessel (total volume 500 mL). The photocatalyst (0.2 g) was spread over ~8 cm<sup>2</sup> on the bottom of a circular glass

dish in the vessel. After sealing the vessel, the air in it was thoroughly replaced by artificial pure air to avoid the disturbance from  $\text{CO}_2$  in air. Gaseous 2-propanol was injected into the vessel with initial concentration of  $\sim 650$  ppm. Before absorption balance of 2-propanol on the photocatalysts, the vessel was kept in dark. Under simulated sunlight irradiation (AM 1.5G,  $100 \text{ mw}\cdot\text{cm}^{-2}$ ), the photocatalytic decomposition process of 2-propanol was essentially divided into two stages:  $(\text{CH}_3)_2\text{CHOH} \rightarrow \text{CH}_3\text{COCH}_3 \rightarrow \text{CO}_2$ . For testing the production yields, gaseous sample (0.5 mL) in each time was extracted from the vessel and injected into a gas chromatograph (GC-14B, Shimadzu) to analysis.

#### 4. Supplementary Data

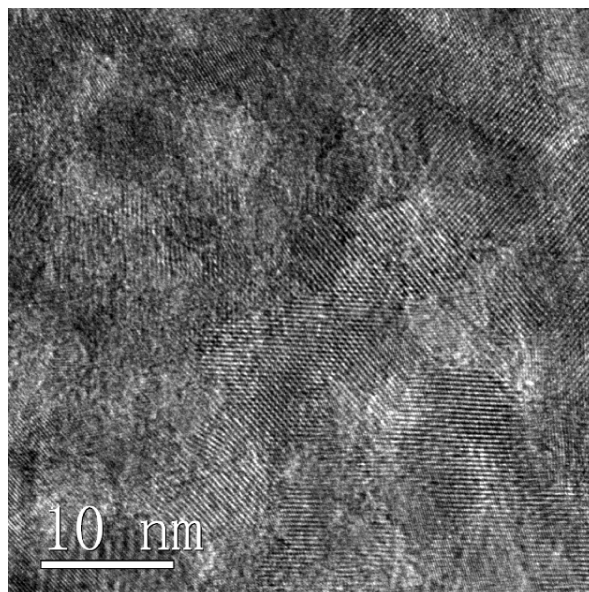


**Figure S1.** HRTEM image of  $\text{TiO}_2$  NCs.

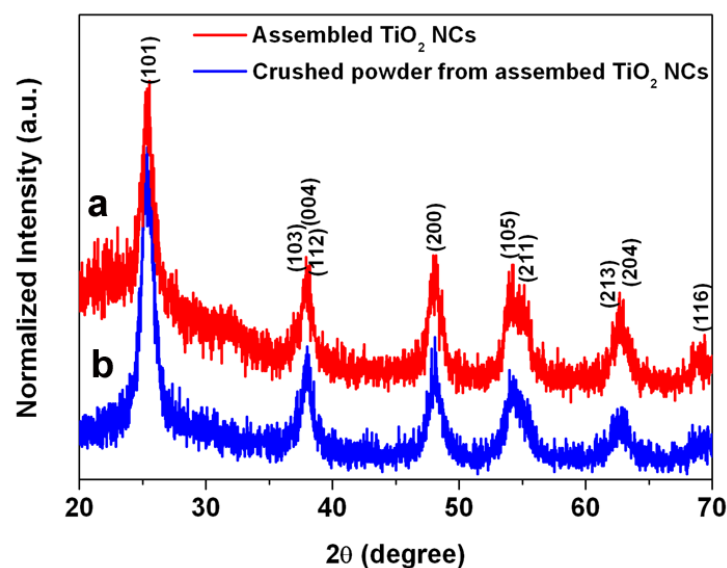


**Figure S2.** XRD patterns: **a**, assembled  $\text{TiO}_2$  NCs; **b**, crushed power from assembled  $\text{TiO}_2$  NCs. This  $\text{TiO}_2$  is indexed to be anatase phase, referred to JCPDS No. 12-1272.

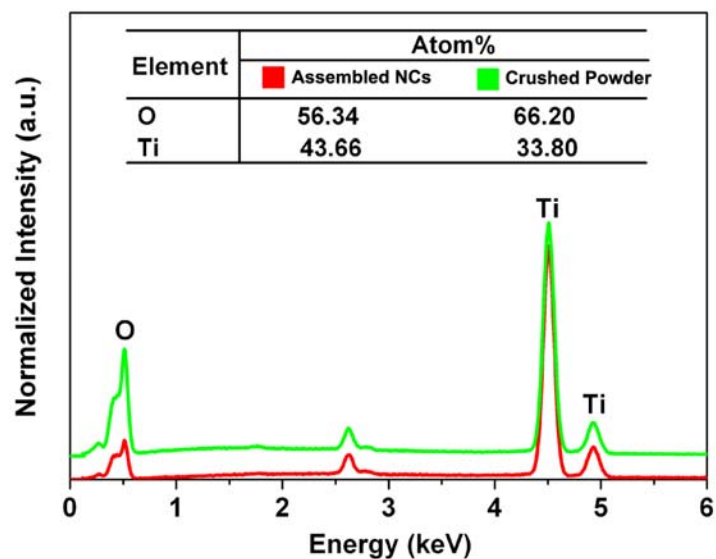


**Figure S3.** EDS spectra of assembled  $\text{TiO}_2$  NCs and crushed power from the assembled  $\text{TiO}_2$  NCs.

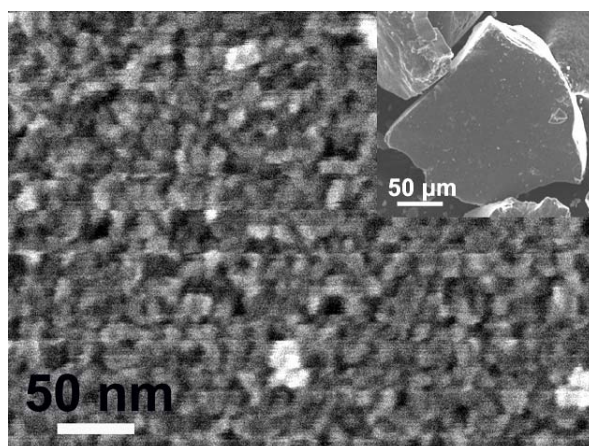


**Figure S4.** SEM image of a bulk of assembled  $\text{TiO}_2$  NCs. Top viewing on a selected surface; inset is a low-magnification image.

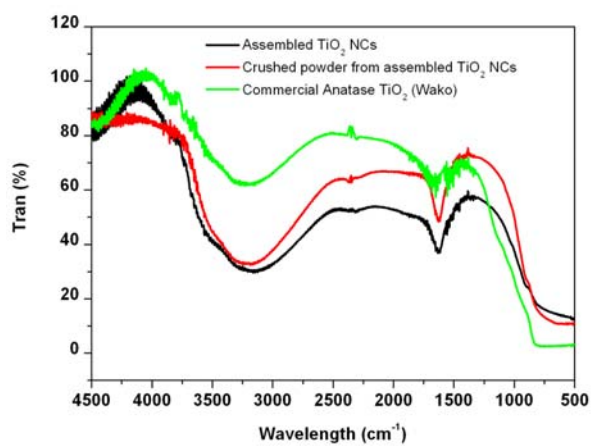


**Figure S5.** Infrared (IR) spectra of assembled TiO<sub>2</sub> NCs, crushed powder and standard anatase TiO<sub>2</sub> (wako).

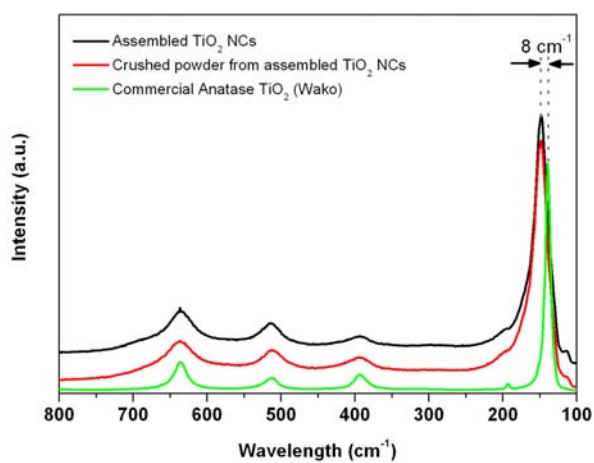


**Figure S6.** Raman spectra of assembled TiO<sub>2</sub> NCs, crushed powder and standard anatase TiO<sub>2</sub> (wako).

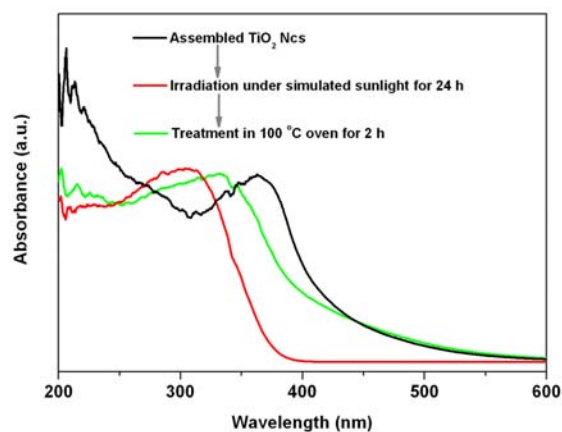


**Figure S7.** UV-vis absorption spectra of the assembled TiO<sub>2</sub> NCs: as prepared; after being irradiated under simulated sunlight for 24 h; and after being treated at 100 °C for 2 h.

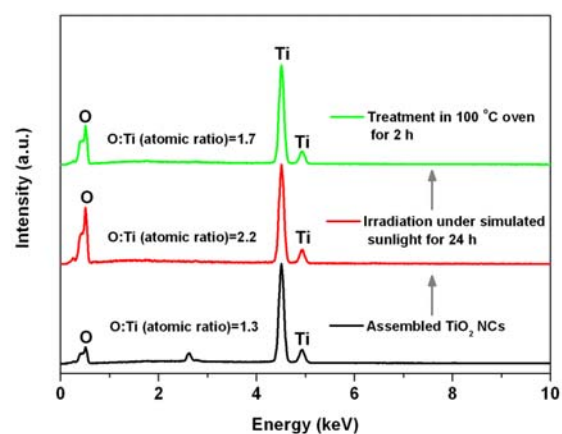


**Figure S8.** UV-vis absorption spectra of the assembled TiO<sub>2</sub> NCs: as prepared; after being irradiated under simulated sunlight for 24 h; and after being treated at 100 °C for 2 h.

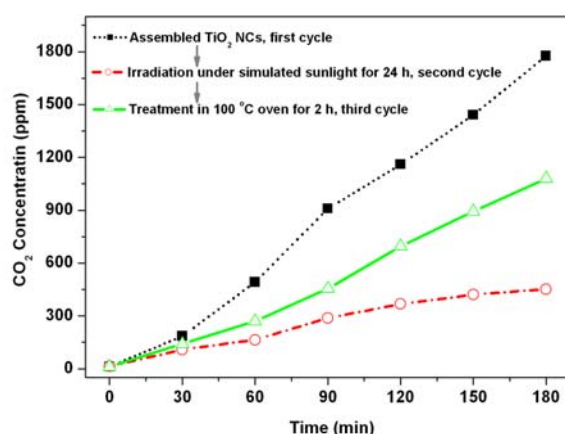


**Figure S9.** CO<sub>2</sub> evolution from decomposition of 2-propanol over the assembled TiO<sub>2</sub> NCs under simulated sunlight irradiation: as prepared (first cycle); after being irradiated under simulated sunlight for 24 h, (second cycle); and after being treated at 100 °C for 2 h (third cycle).

## 5. Details of theoretical calculations

Our electronic structure calculations were based on the density-functional theory (DFT) +*U* approach.<sup>1</sup> The exchange-correlation energy functional was represented by the local density approximation (LDA) proposed.<sup>2</sup> Projector-augmented wave pseudopotentials were employed as implemented in the VASP code.<sup>3,4</sup> The valence configurations of the pseudo-potentials were  $3p^63d^34s^1$  for Ti and  $2s^22p^4$  for O. The energy cutoff for the plane-wave basis set expansion was set at 500 eV. A Monkhorst-Pack k-point set of  $2 \times 2 \times 1$  was used. We applied *U* to Ti *d* and O *p* ( $U(\text{Ti } d) = 10.77$  eV and  $U(\text{O } p) = 6.27$  eV) which were determined so as to reproduce the experimental band gap (3.2 eV). The importance of applying *U* to O *p* as well as Ti *d* states was discussed elsewhere.<sup>5</sup> The optimized lattice parameters of bulk anatase TiO<sub>2</sub> are in good agreement with those of experiments (Table S1).

In Model A (Figure Xa), two ideal (101) surface of anatase TiO<sub>2</sub>, which is based two slabs with 12-layers each, are faced with a symmetry in which one surface is slid in the plane toward (0.5,0.5) direction of the lattice vectors with respect to the other surface. This results in 144-atoms supercell. The initial distance between the two surfaces was set to 1 Å. The fifth to eighth layers were fixed during relaxations to represent bulk region. In model B (Figure Xb), one oxygen atom was removed from each surface per unit. To compare the stability of oxygen vacancies at interface and on surface, we have also performed calculations for open surfaces with and without oxygen vacancies at the outer most layer where a vacuum region was introduced with the same thickness as 12-layers of TiO<sub>2</sub>.

**Table S1.** Lattice constants for TiO<sub>2</sub> determined by LDA+*U* compared to experimental values (Ref. 6).

Lattice parameters	Theory	Experiment <sup>a</sup>
a(Å)	3.88	3.78216
c(Å)	9.65	9.50226
d <sub>eq</sub> (Å)	1.98	1.9322
d <sub>ap</sub> (Å)	2.01	1.9788
u (Å)	0.208	0.20824

<sup>a</sup>Reference 6

## References

1. V. I. Anisimov, J. Zaanen, and O. K. Andersen, *Phys. Rev. B*, 1991, **44**, 943-954.
2. J. P. Perdew, and A. Zunger, *Phys. Rev. B*, 1981, **23**, 5048-5079.
3. G. Kresse, and J. Hafner, *Phys. Rev. B*, 1993, **47**, 558-561.
4. G. Kresse, and J. Furthmüller, *Phys. Rev. B*, 1996, **54**, 11169-11186.
5. B. J. Morgan, and G. W. Watson, *Phys. Rev. B*, 2009, **80**, 233102.
6. J. K. Burdett, T. Hughbanks, G. J. Miller, J. W. Richardson, Jr., and J. V. Smith, *J. Am. Chem. Soc.*, 1987, **109**, 3639-3646.